Communication: Control of chemical reactions using electric field gradients

Shivaraj D. Deshmukh and Yoav Tsori[a)]
Department of Chemical Engineering, Ben-Gurion University of the Negev, Beer-Sheva 84105, Israel

(Received 28 March 2016; accepted 10 May 2016; published online 19 May 2016)

We examine theoretically a new idea for spatial and temporal control of chemical reactions. When chemical reactions take place in a mixture of solvents, an external electric field can alter the local mixture composition, thereby accelerating or decelerating the rate of reaction. The spatial distribution of electric field strength can be non-trivial and depends on the arrangement of the electrodes producing it. In the absence of electric field, the mixture is homogeneous and the reaction takes place uniformly in the reactor volume. When an electric field is applied, the solvents separate and the reactants are concentrated in the same phase or separate to different phases, depending on their relative miscibility in the solvents, and this can have a large effect on the kinetics of the reaction. This method could provide an alternative way to control runaway reactions and to increase the reaction rate without using catalysts. *Published by AIP Publishing.* [http://dx.doi.org/10.1063/1.4951709]

Chemical reactions are conventionally controlled by pressure, temperature, surface area, concentration, or by using a catalyst.[1,2] Attention has turned to active modification of molecular collision processes[3] and to the manipulation of activation energy barriers.[4,5] Lasers were used for selectively making and breaking chemical bonds[6] and current research looks at ways to exploit ultrafast lasers for mode-selective chemistry, stereodynamic, and quantum control of molecular processes[3,7,8] in cost effective ways. Electric[9–11] and magnetic fields and ultrasound are also used to control molecular collisions and thereby the chemistry.[12,13] Electric and magnetic fields modify the orientation of molecules and may change the ion and molecular transport rates, they can modify the quantum states of molecules,[12,13] and they may lead to Stark and Zeeman shifts in the energy levels. In addition, large electric fields at charged metal surfaces are important in the chemisorption of atoms and molecules.[14]

Here we propose a new direction for spatial and temporal control of chemical reactions. Our idea relies on the use of a mixture of two or more solvents. Reactions taking place in such a mixture are influenced by the composition of the solvents. An external field can lead to "electro-prewetting" transition of the solvents even when their initial state is homogeneous.[15,16] In this transition, the solvents separate from each other and migrate to locations that minimize the total free energy of the mixture and depend on the electrode design. An interface thus appears separating the formed domains.

There are now two scenarios and for clarity we focus on a binary mixture of solvents and two reactants. In the first, due to their Gibbs transfer energy, the reactants are more miscible in the same solvent. In that case field-induced demixing will lead to concentration of the reactants in a small volume and to accelerated reaction kinetics compared to the no-field, homogeneous state. The product will be initially produced in the same small volume. In the second scenario, the two reactants are preferentially miscible in different solvents. In that case, the reaction will take place at the interface separating liquid domains. This interfacial reaction is expected to be slowed down compared to the no-field (homogeneous) state. The product will initially be created at the interface between coexisting domains. In both cases, switching off the field will allow re-mixing of the solvents and return to the homogeneous state and to "normal" kinetics.

Thermodynamics of liquid mixtures is underlying the reactions in electric fields. Consider for simplicity a mixture of two solvents. The total free energy of the mixture is given on the mean-field level as

$$\mathcal{F} = \int_\Omega [f_m(\phi,T) + f_e(\phi,\mathbf{E}) + f_i(\phi,T)]\, d\Omega, \qquad (1)$$

where Ω is the volume occupied by the mixture. The volume fraction of solvent 1 is given by ϕ and the volume fraction of solvent 2 is $1-\phi$, T is temperature, and f_m, f_e, and f_i are mixing, electrostatic, and interfacial energies. The mixing free energy per unit volume is given by $f_m = (k_BT/v_0)[\phi\log\phi + (1-\phi)\log(1-\phi) + \chi\phi(1-\phi)]$, where k_B is the Boltzmann constant and v_0 is a molecular volume assumed here to be equal for the two solvents.[17,18] χ is the Flory parameter varying inversely with T: $\chi \sim 1/T$. For positive values of χ, the phase diagram has upper critical solution temperature[19] and the critical point is given by $(\phi_c,\chi_c) = (1/2,2)$. For such symmetric free energy expressions, the binodal curve $T_b(\phi)$ in the ϕ-T phase diagram is given by $\partial f(\phi,T_b)/\partial\phi = 0$. Above this curve, the mixture is stable in the homogeneous phase. A quench to temperatures T below T_b leads to phase separation of two coexisting phases with compositions given by the values of the binodal at T.

The interfacial free energy density is given by $f_i = (k_BT/2v_0)\chi\lambda^2|\nabla\phi|^2$, where λ is a constant related to interface width.[18] The electrostatic free energy density is given by $f_e = -(1/2)\epsilon_0\epsilon(\phi)|\nabla\psi|^2$, where ϵ_0 is the permittivity of free space, ϵ is the relative permittivity of the mixture

a)tsori@bgu.ac.il

Reuse of AIP Publishing content is subject to the terms: https://publishing.aip.org/authors/rights-and-permissions. Downloaded to IP: 37.142.72.218 On: Thu, 19 May 2016 14:53:06

depending on its relative composition, and $\psi(\mathbf{r})$ is the local electric potential.

In order for the electric field to be effective in separating the liquids, it must have large spatial gradients. We chose the simple "wedge" geometry to illustrate the concept of chemical reactions. The wedge is comprised of two flat and conducting plates oriented with an opening angle β between them ($\beta = 0°$ corresponds to a parallel-plate capacitor). In this effectively two-dimensional system, the electric field depends only on the distance r from the imaginary meeting point of the plates and is oriented in the azimuthal $\hat{\theta}$ direction.[20]

In the wedge geometry chosen, all quantities depend on r alone and the hydrodynamic flow velocity $\mathbf{v}$ vanishes. The equations governing the demixing dynamics are then[20,21]

$$\frac{\partial \phi}{\partial t} = D\nabla^2 \frac{\delta f}{\delta \phi}, \quad \nabla \cdot [\epsilon(\phi)\nabla\psi] = 0, \tag{2}$$

where $f = f_m + f_i + f_e$ is the total mixture free energy density and D is an Onsager diffusivity constant taken here to be independent of ϕ.

We consider a simple irreversible reaction $A + B \xrightarrow{k} 2C$, where molecules of compounds A and B react to give product C and k is the rate constant. When the reaction takes place in a mixture of two solvents, each molecule A, B, and C feels a spatially dependent potential that depends on its relative solubility denoted by u_a, u_b, and u_c, respectively. For the A molecule $u_a(\mathbf{r}) = u_1^a\phi + u_2^a(1-\phi)$ and similar expressions for $u_b(\mathbf{r})$ and $u_c(\mathbf{r})$. The parameters u_1^a ad u_2^a indicate the solubilities of compound A in liquids 1 and 2, respectively. The difference in the solubility parameters $\Delta u^a = u_2^a - u_1^a$ is related to the Gibbs transfer energy ΔG_t for transferring one A molecule from a solvent with composition ϕ_1 to a solvent with composition ϕ_2 via $\Delta G_t = \Delta u^a(\phi_2 - \phi_1)$. Experiments show that G_t is on the order of $1 - 10k_BT$ in aqueous mixtures[22] and hence $\Delta u^a \sim 1 - 10$.

The mass balance of compound A gives the modified reaction-diffusion equation: $\partial C_a/\partial t = D_a\nabla^2 C_a + D_a\nabla \cdot [C_a\nabla(u_a/k_BT)] - kC_aC_b$. Here D_a is the diffusion coefficient of compound A in the mixture, assumed to be independent of T and ϕ. This equation can be recast in dimensionless form

$$\frac{\partial \tilde{C}_a}{\partial \tilde{t}} = \tilde{\nabla}^2\tilde{C}_a + \tilde{\nabla}\cdot\left(\tilde{C}_aU_a'\tilde{\nabla}\phi\right) - \tilde{k}\tilde{C}_a\tilde{C}_b, \tag{3}$$

where $\tilde{C}_a = C_a/C_{a0}$ is the concentration scaled by C_{a0}, the initial (uniform) concentration of A molecules, $\tilde{k} = kC_{a0}R_1^2/D_a$ is a scaled reaction rate, and $U_a' = (u_2^a - u_1^a)/k_BT$. The length is scaled using R_1 (the minimal distance r from the imaginary meeting point of the plates): $\tilde{r} = r/R_1$, and time is scaled via $\tilde{t} = D_a/R_1^2 t$. When a potential difference of magnitude V is applied across wedge electrodes, the ratio of the electrostatic energy stored in a molecular volume v_0 to the thermal energy is given by the dimensionless number[23] $M_w \equiv V^2v_0\epsilon_0/(4\beta^2k_BT_cR_1^2)$, where T_c is the critical temperature. Similar mass balance equation can be written for compounds B and C,

$$\frac{\partial \tilde{C}_b}{\partial \tilde{t}} = \frac{D_b}{D_a}\left[\tilde{\nabla}^2\tilde{C}_b + \tilde{\nabla}\cdot\left(\tilde{C}_bU_b'\tilde{\nabla}\phi\right)\right] - \tilde{k}\tilde{C}_a\tilde{C}_b, \tag{4}$$

$$\frac{\partial \tilde{C}_c}{\partial \tilde{t}} = \frac{D_c}{D_a}\left[\tilde{\nabla}^2\tilde{C}_c + \tilde{\nabla}\cdot\left(\tilde{C}_cU_c'\tilde{\nabla}\phi\right)\right] + 2\tilde{k}\tilde{C}_a\tilde{C}_b, \tag{5}$$

with $\tilde{C}_b = C_b/C_{a0}$, $\tilde{C}_c = C_c/C_{a0}$, $U_b' = (u_2^b - u_1^b)/k_BT$, and $U_c' = (u_2^c - u_1^c)/k_BT$.

In this paper, we assume that the reaction is slow compared to the kinetics of phase separation. If this condition holds, the initially homogeneous mixture phase-separates on a fast time scale to two coexisting domains with uniform densities of the reactants. The composition $\phi(\mathbf{r})$ attains its equilibrium profile, minimizing the sum of mixture, interfacial, and electrostatic energies. On a much longer scale, the chemical reaction then proceeds, with the compounds A, B, and C experiencing a spatially dependent force derivable from the u's as is explained above. We further distinguish between the two cases whether the molecules A and B prefer the same phase or not.

Reactants A and B prefer the same phase. Figures 1(a)-1(c) show concentration profiles at various times when the reactants and product prefer the more polar phase (high value of ϕ). At $\tilde{t} = 0$ the mixture has two coexisting domains with an interface at $r/R_1 \simeq 2.5$. As time progresses, the A and B molecules diffuse towards the more polar region ($r/R_1 < 2.5$, large ϕ) and sharp gradient occurs at the interface between the coexisting phases. The concentrations of A and B molecules are the same because we took $U_a' = U_b'$. As time increases, A and B continue to diffuse to the polar solvent but on the same time are consumed due to the reaction and the creation of C. At long times $\tilde{C}_a$ and $\tilde{C}_b$ become very small; the concentration of C obeys the Boltzmann's distribution and is found preferentially in the polar phase where it is more soluble.

In Figure 1(d), we calculate the spatially averaged product amount $\bar{C}_c \equiv \Omega^{-1}\int \tilde{C}_c d\Omega$ vs time. We compare the case with electric field and two coexisting domains (lines) with the zero-field case and a homogeneous mixture (lines with symbols), for constant electric field and varying reaction rates $\tilde{k}$. As can be seen, the electric field increases the effective rate of the reaction. It does so more effectively for the slow reactions (small values of $\tilde{k}$) and less effectively for the fast reactions (large values of $\tilde{k}$). Irrespective of $\tilde{k}$, material conservation dictates that $\bar{C}_c \to 2$ when $\tilde{t} \to \infty$.

Fig. 2 examines how the effective reaction rate depends on the magnitude of the external potential. A phase-separation transition occurs when the applied voltage in the wedge is larger than the critical value, which depends on the temperature and mixture composition. When the voltage increases past this threshold, the "contrast" between the phases increases (ϕ increases at small values of r and decreases for large values of r) and the interface displaces to larger values of r. Three profiles of ϕ for different values of the potential are shown in the inset. As can be seen, $\bar{C}_c$ is larger with increasing potential. However, an increase of M_w from 0.036 to 0.144 has only a modest effect on $\bar{C}_c$. Indeed, even a hypothetical infinite potential would lead to a finite effective reaction rate.

The preferential solubility of the reactants in the solvents is an important factor determining the rate of the reaction. In Fig. 3, we plot $\bar{C}_c$ for different solubility values at a fixed value of M_w. While the asymptotic behavior at long

Reuse of AIP Publishing content is subject to the terms: https://publishing.aip.org/authors/rights-and-permissions. Downloaded to IP: 37.142.72.218 On: Thu, 19 May 2016 14:53:06

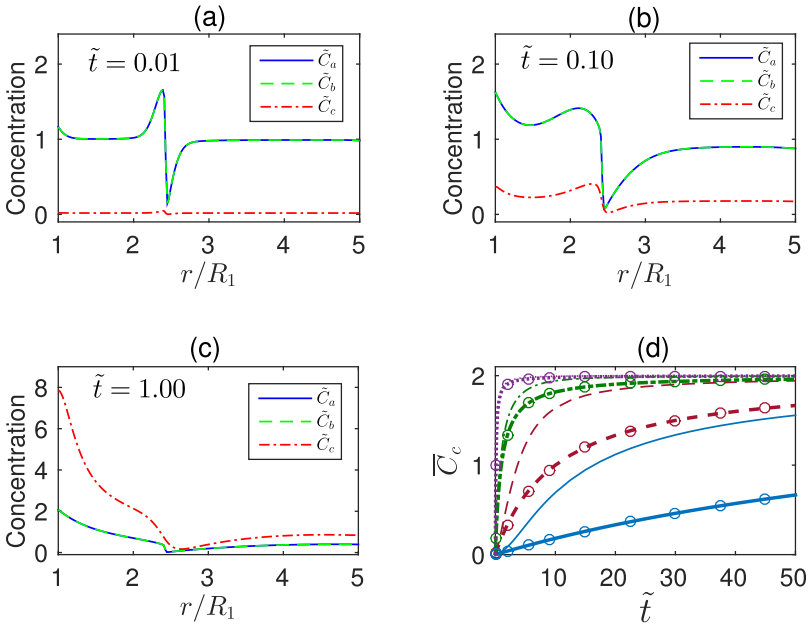

FIG. 1. Concentration profiles $\tilde{C}_a$, $\tilde{C}_b$, and $\tilde{C}_c$ vs time when both A and B molecules are soluble in the polar phase. (a)-(c) Temporal progression obtained from a numerical solution of Eqs. (3)–(5). (d) Volume-average product $\bar{C}_c$ vs time for varying values of $\tilde{k}$. Solid, dashed, dashed-dotted, and dotted lines correspond to $\tilde{k} = 0.01$, 0.1, 1, 10, respectively. Circles are the same but without field. The solubility potentials are $U'_a = U'_b = U'_c = 10$, the diffusion constants are $D_a = D_b = 100 \times D_c$, the average mixture composition is $\phi_0 = 0.33$, the dimensionless electric potential is $M_w = 0.144$, and the dimensionless reaction rate is $\tilde{k} = 1$.

times dictates $\bar{C}_c \to 2$ clearly, the dynamics are faster as the solubility difference increases.

Reactants A and B prefer different phases. We turn to the interesting case where the reactants are "antagonistic" in the sense that they prefer different solvents. Figure 4 shows the concentration profiles vs time and should be compared to Fig. 1. As before, $\tilde{C}_a$ and $\tilde{C}_b$ start from a uniform distribution at $\tilde{t} = 0$. But here they diffuse in opposite directions—A to the polar solvent at small r's and B to the less polar solvent at large r's. At early times the gradients in $\tilde{C}_a$ and $\tilde{C}_b$ occur at the interface between the solvents. The profiles evolve in time; as the reactants migrate according to their solubility, they are consumed and C is created. In this calculation, we assumed that the product is equally soluble in both solvents and thus at long times $\tilde{C}_c$ is uniform. Far from the interface, in the bulk liquid, the transport of A and B is mainly due to diffusion (first term in the right-hand side of Equations (3) and (4)). Near an interface the high gradient in ϕ leads to a large force from the solubility potential and transport is dominated by the solubility difference (second term in the right-hand side of Equations (3) and (4)).

In Fig. 4(d), we plot the average product $\bar{C}_c$ vs time for different values of the potential. In contrast to Fig. 1(d) here the effective reaction is *slower* with field (lines) as compared to the no-field case (lines with symbols). As in Fig. 1(d), fast reactions are less affected by the field (large values of $\tilde{k}$). The total product $\tilde{C}_c$ tends to 2 due to mass conservation.

The effective slowing-down of the reaction saturates with the magnitude of the applied potential, see Fig. 5. As M_w increases ($M_w \propto V^2$), the more polar solvent is pulled to the region with higher electric field, thereby raising the value of ϕ at small r's and reducing it at large r's (low electric field region). Curves show $\tilde{C}_c$ vs time for different values of M_w. All curves increase from $\tilde{C}_c = 0$ at $\tilde{t} = 0$ to $\tilde{C}_c = 2$ at infinity. Curves exhibit an early increase on a small time scale dictated by diffusion over the mesoscopic width of the interface between coexisting phases. After the rapid increase, the curves increase slowly on a time scale dictated by diffusion over the macroscopic size of the wedge.

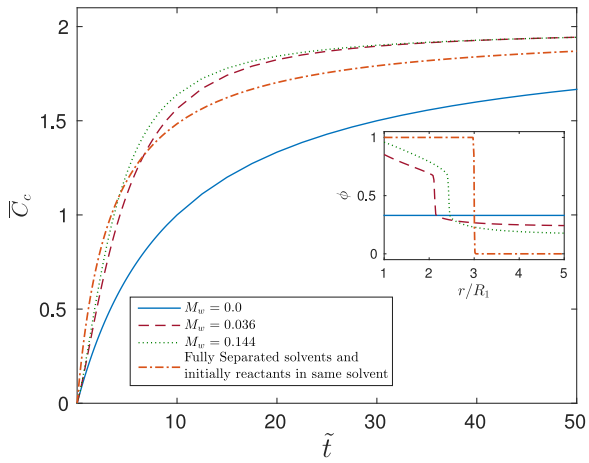

FIG. 2. Dependence of the average product concentration $\bar{C}_c$ on the applied electric potential M_w. Inset shows the mixture profiles for the same M_w's. $U'_a = U'_b = 10$, $\phi_0 = 0.33$, and $\tilde{k} = 0.1$.

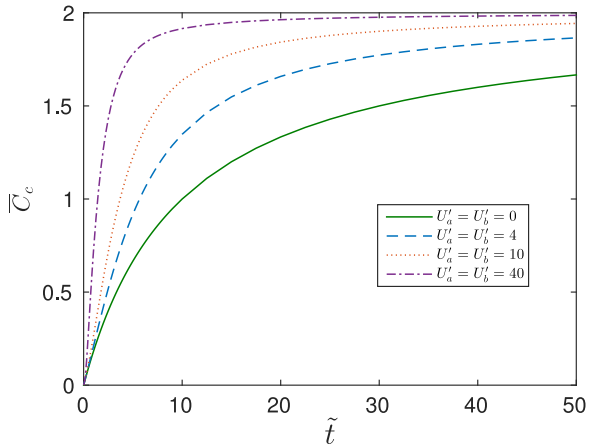

FIG. 3. Dependence of the average product concentration $\bar{C}_c$ on the solubility parameters. $\phi_0 = 0.33$, $M_w = 0.144$, and $\tilde{k} = 0.1$.

Reuse of AIP Publishing content is subject to the terms: https://publishing.aip.org/authors/rights-and-permissions. Downloaded to IP: 37.142.72.218 On: Thu, 19 May 2016 14:53:06

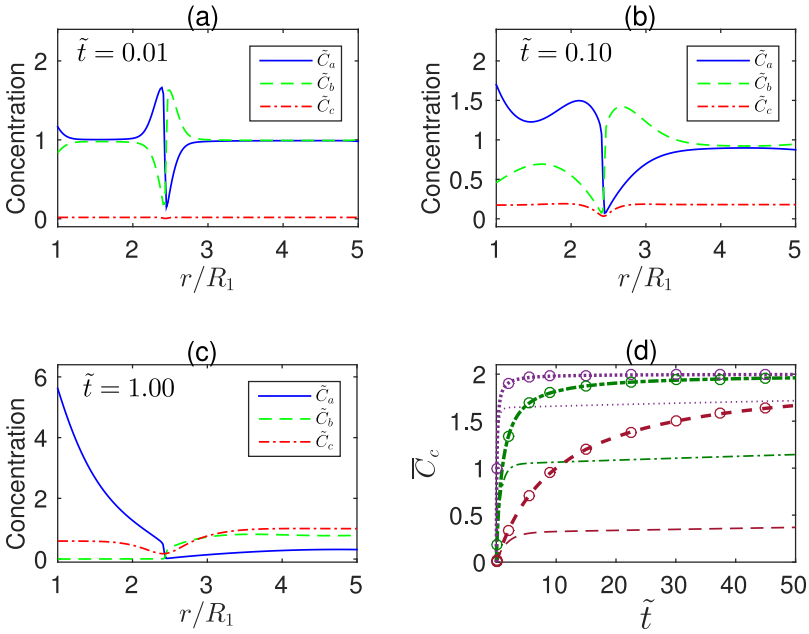

FIG. 4. Concentration profiles $\tilde{C}_a$, $\tilde{C}_b$, and $\tilde{C}_c$ and average product $\bar{C}_c$ for the same conditions as in Fig. 1 except that molecule A is soluble in the polar phase and B in the less polar phase: $U'_a = 10$ and $U'_b = -10$.

The overall reaction rate is slowed down when the reactants are preferentially soluble in different solvents, as can be seen in Fig. 6. Clearly the electric potential is crucial here because in its absence the mixture is homogeneous and with it two domains exist. All curves in the figure start from zero and increase to 2 at long times. Here again there are two time scales – a fast transient corresponding to diffusion over the interface, accompanied by a slow relaxation dictated by diffusion over macroscopic lengths. The stronger the incompatibility between the reactants the larger the difference in concentration of A and B molecules in the two domains and the slower is the overall relaxation.

In Fig. 7, we show the non-trivial dependence of the rate of reaction on the average mixture composition ϕ_0. At a fixed temperature and electric potential and for values of ϕ_0 smaller than the critical value, an increase in ϕ_0 to values closer to the binodal curve leads to an increase in the location of the interface between the polar and less polar phases (inset). However, at the same time, the "contrast" between the phases diminishes and the thickness of the interface increases. As a result, for the values presented in this calculation, at long times the reaction which is slowest is the one with intermediate value, $\phi_0 = 0.2$, and not one of the extreme values $\phi_0 = 0.1$ or $\phi_0 = 0.4$.

In summary, electric field gradients can control the effective reaction rate in reactions taking place in mixtures of solvents. Whether the reaction in the "on" state is faster or slower than in the "off" state depends on whether the reactants are miscible in the same solvent or in different ones. The effective reaction rate depends sensitively on the electric potential, mixture composition, and distance from the binodal curve of the mixture and is independent of the preferential solvation of the product C. We believe that this method could provide an alternative way to control runaway reactions and to increase the reaction rate without using catalysts.

In the current study, we assumed that the liquid flow due to phase separation is very fast compared to the reaction

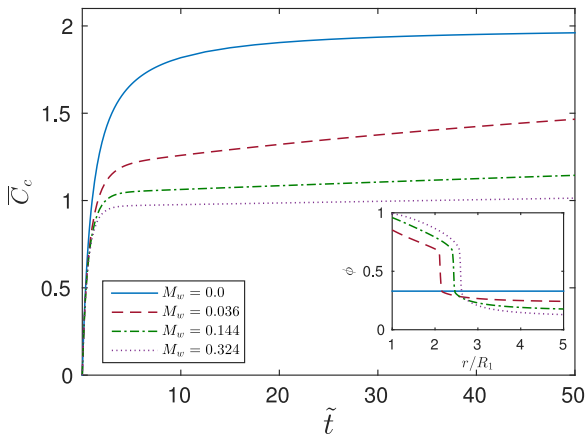

FIG. 5. The influence of the electric potential M_w on the average product concentration $\bar{C}_c$. Larger values of M_w decrease the effective reaction rate. Inset shows the equilibrium profiles $\phi(r)$ for the same M_w's. $U'_a = 10$, $U'_b = -10$, $\phi_0 = 0.33$, and $\tilde{k} = 1$.

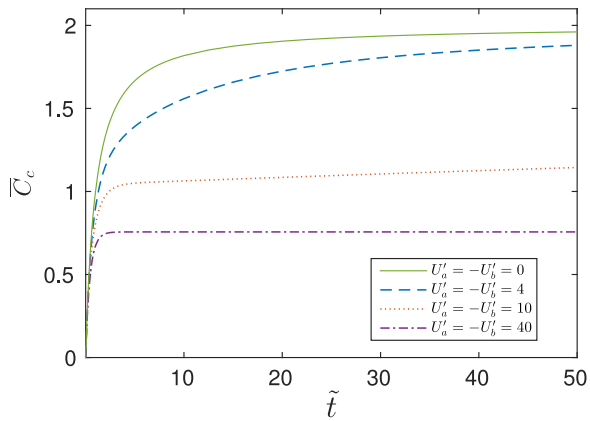

FIG. 6. The influence of the preferential solubility of A and B molecules on the average total product $\bar{C}_c$. The reaction is considerably slowed down as $|U'_a|$ and $|U'_b|$ increase. $\phi_0 = 0.33$, $M_w = 0.144$, and $\tilde{k} = 1$.

Reuse of AIP Publishing content is subject to the terms: https://publishing.aip.org/authors/rights-and-permissions. Downloaded to IP: 37.142.72.218 On: Thu, 19 May 2016 14:53:06

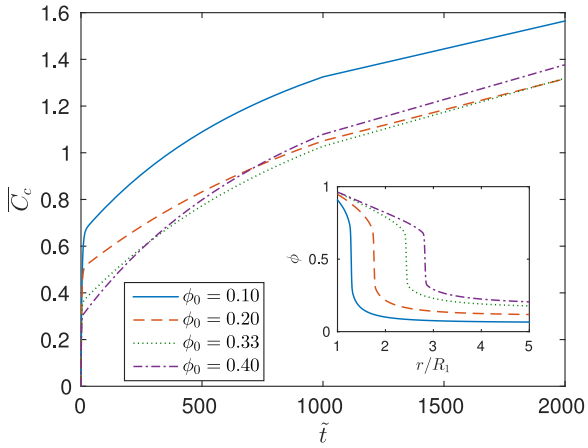

FIG. 7. Influence of the average mixture composition ϕ_0 on the average total product $\bar{C}_c$ at a fixed electric potential given by $M_w = 0.144$, solubilities $U'_a = -U'_b = 10$ and $\tilde{k} = 0.1$. Inset is the equilibrium profiles $\phi(r)$ for the same values of ϕ_0.

kinetics but it may be interesting to relax this assumption. Electric fields are especially suited for use in microfluidic devices where they have been used to transport liquids in small channels. Such systems pose great promise for field-induced chemical reactions. Indeed, the challenge is to better understand how reactions are coupled with flow, either from pressure gradients in the channel or from the phase-separation itself. Future work will also consider ionic reagents, mixtures that have a lower critical solution temperature (e.g., water and 2,6 lutidine),[24] and reversible reactions. In such reactions, the preferential solubility of C is important and the effective reaction rate can increase or decrease depending on whether C is soluble in the same solvent as A and B or not.

This work was supported by the European Research Council "Starting Grant" No. 259205, COST Action MP1106, and Israel Science Foundation Grant No. 56/14.

[1]K. Sanderson, Nature **469**, 18 (2011).
[2]P. Atkins and J. de Paula, *Atkins' Physical Chemistry* (Oxford University Press, Oxford, 2006).
[3]P. Brumer and M. Shapiro, Annu. Rev. Phys. Chem. **43**, 257 (1992).
[4]L. Ratschbacher, C. Zipkes, C. Sias, and M. Kohl, Nat. Phys. **8**, 649 (2012).
[5]C. Y. Tseng, A. Wang, and G. Zocchi, Europhys. Lett. **91**, 18005 (2010).
[6]A. Assion, T. Baumert, M. Bergt, T. Brixner, B. Kiefer, V. Seyfried, M. Strehle, and G. Gerber, Science **282**, 919 (1998).
[7]R. N. Zare, Science **279**, 1875 (1998).
[8]B. J. Sussman, D. Townsend, M. Y. Ivanov, and A. Stolow, Science **314**, 278 (2006).
[9]M. Tachiya, J. Chem. Phys. **87**, 4622 (1987).
[10]M. Hilczer, S. Traytak, and M. Tachiya, J. Chem. Phys. **115**, 11249 (2001).
[11]S. Y. Reigh, K. J. Shin, and H. Kim, J. Chem. Phys. **132**, 164112 (2010).
[12]M. Lemeshko, R. V. Krems, J. M. Doyle, and S. Kais, Mol. Phys. **111**, 1648 (2013).
[13]M. Brouard, D. H. Parker, and S. Y. T. van de Meerakker, Chem. Soc. Rev. **43**, 7279 (2014).
[14]H. Kreuzer, Surf. Sci. **246**, 336 (1991).
[15]Y. Tsori, F. Tournilhac, and L. Leibler, Nature **430**, 1 (2004).
[16]Y. Tsori, Rev. Mod. Phys. **81**, 1471 (2009).
[17]M. Doi, *Introduction to Polymer Physics* (Oxford University Press, Oxford, 1996).
[18]S. A. Safran, *Statistical Thermodynamics of Surfaces, Interfaces, and Membranes* (Westview Press, New York, 1994).
[19]P. Debye and K. Kleboth, J. Chem. Phys. **42**, 3155 (1965).
[20]J. Galanis and Y. Tsori, J. Chem. Phys. **140**, 124505 (2014).
[21]T. Imaeda, A. Furukawa, and A. Onuki, Phys. Rev. E **70**, 051503 (2004).
[22]Y. Marcus, *Ion Solvation* (Wiley, New York, 1985).
[23]S. Samin and Y. Tsori, J. Chem. Phys. **131**, 194102 (2009).
[24]S. Samin, M. Hod, E. Melamed, M. Gottlieb, and Y. Tsori, Phys. Rev. Appl. **2**, 024008 (2014).

Reuse of AIP Publishing content is subject to the terms: https://publishing.aip.org/authors/rights-and-permissions. Downloaded to IP: 37.142.72.218 On: Thu, 19 May 2016 14:53:06